Role of Strong Correlation in the Recent Angle-Resolved Photoemission Spectroscopy Experiments on Cuprate Superconductors

S. Yunoki,[1] E. Dagotto,[2,3] and S. Sorella[1]

[1]*Istituto Nazionale per la Fisica della Materia and International School for Advanced Studies, via Beirut 4, 34014 Trieste, Italy*
[2]*Department of Physics and Astronomy, The University of Tennessee, Knoxville, Tennessee 37996-1200, USA*
[3]*Condensed Matter Sciences Division, Oak Ridge National Laboratory, Oak Ridge, Tennessee 37831-6393, USA*

(Received 1 October 2004; published 24 January 2005)

Motivated by recent photoemission experiments on cuprates, the low-lying excitations of a strongly correlated superconducting state are studied numerically. It is observed that along the nodal direction these low-lying one-particle excitations show a linear momentum dependence for a wide range of excitation energies and, thus, they do not present a kinklike structure. The nodal Fermi velocity v_F, as well as other observables, are systematically evaluated directly from the calculated dispersions, and they are found to compare well with experiments. It is argued that the parameter dependence of v_F is quantitatively explained by a simple picture of a renormalized Fermi velocity.

DOI: 10.1103/PhysRevLett.94.037001 PACS numbers: 74.20.Mn, 71.10.Fd, 71.10.Li

Since the discovery of the copper-based high-T_c superconductors [1], there have been extensive studies, both experimentally and theoretically, to understand the origin of the superconductivity as well as the unusual normal state properties [2]. This vast effort has proved that among the many experimental techniques angle-resolved photoemission spectroscopy (ARPES) is one of the most powerful tools, since it can provide important microscopic information of the electronic structure of these materials [3]. One of the recent key findings by ARPES experiments concerns the low-lying electronic excitations in the $(0, 0)$ to (π, π) direction (nodal direction) of the Brillouin zone: (i) the low-lying dispersion shows a kink at an energy in the range 50–80 meV from the Fermi level [4,5], and (ii) the nodal Fermi velocity shows almost no doping dependence within the experimental error bars ($\sim 1.8 \pm 0.4$ eV Å) for a wide range of hole concentrations x ($0 < x \lesssim 0.2$–0.3) [6]. To explain the peculiar feature (i), the idea that electrons could be strongly coupled to other degrees of freedom, such as phonons and magnetic fluctuations, has been introduced [5]. This can naturally explain the appearance of a new energy scale. There are already theoretical studies in this direction [7]. However, the kink structure origin is still under debate. Regarding feature (ii), there has been no consensus on its origin. We believe that before studying more complicated models it is important to understand to what extent a purely electronic model alone can explain these features observed experimentally. This is precisely the main purpose of this Letter.

In this Letter, using a variational Monte Carlo (MC) method, the low-lying excitations of a strongly correlated superconducting state with d-wave pairing symmetry are studied. By directly calculating the excitation spectrum, it is found that the low energy one-particle excitations in the nodal direction show a linear momentum dependence, instead of a kinklike structure. Our detailed and systematic calculations for the nodal Fermi velocity v_F, as well as a coupling strength λ defined below, reveal that in spite of not having a kink structure in $\varepsilon(\mathbf{k})$, the doping dependence of v_F and λ are nevertheless in good agreement with experiments. Moreover, it is shown that the doping dependence of v_F can be understood quantitatively as a renormalized Fermi velocity.

As a canonical model for the cuprates, here we consider the two dimensional (2D) t-J model on a square lattice described by the following Hamiltonian [8];

$$H = J\sum_{\langle i,j\rangle}(\mathbf{S}_i \cdot \mathbf{S}_j - n_i n_j/4) - t\sum_{\langle i,j\rangle\sigma}(c^\dagger_{i,\sigma}c_{j,\sigma} + \text{H.c.}) - t'\sum_{\langle i,j\rangle'\sigma}(c^\dagger_{i,\sigma}c_{j,\sigma} + \text{H.c.}). \quad (1)$$

Here $c^\dagger_{i,\sigma}$ is the creation operator of a spin $\sigma(=\uparrow, \downarrow)$ electron at site i, and $n_i = n_{i,\uparrow} + n_{i,\downarrow}$ and $\mathbf{S}_i = \frac{1}{2}c^\dagger_{i,\alpha}\sigma_{\alpha\beta}c_{i,\beta}$ are the electron density and spin operators. $\langle i, j\rangle$ ($\langle i, j\rangle'$) runs over the (next) nearest-neighboring sites, and no double occupancy is allowed on each site. This model has been studied extensively and found to show a d-wave superconducting regime in its phase diagram [9,10].

It is well known that a Gutzwiller projected BCS wave function with d-wave singlet pairing provides a satisfactory variational state for the 2D t-J model over a wide range of parameters [11]. Here we use a slightly more complex variational wave function [10] defined by $|\Psi^{(N)}_{\text{var}}\rangle = \hat{\mathcal{P}}_N\hat{\mathcal{P}}_G\hat{\mathcal{P}}_J|\text{BCS}\rangle$, where $|\text{BCS}\rangle$ is the BCS ground state wave function, $|\text{BCS}\rangle = \prod_{\mathbf{k}}[1 + f_{\mathbf{k}}c^\dagger_{\mathbf{k}\uparrow}c^\dagger_{-\mathbf{k}\downarrow}]|0\rangle$, $c^\dagger_{\mathbf{k},\sigma}$ the Fourier transform of $c^\dagger_{i,\sigma}$, $\hat{\mathcal{P}}_N$ the projection operator onto the subspace of N electrons, $\hat{\mathcal{P}}_G = \prod_i(1 - n_{i,\uparrow}n_{i,\downarrow})$ the Gutzwiller projection operator, $\hat{\mathcal{P}}_J = \exp(\sum_{i,j}\alpha^{ij}_{\text{var}}n_i n_j)$ a Jastrow factor, and $f_{\mathbf{k}} = \Delta_{\mathbf{k}}/(\xi_{\mathbf{k}} - \mathcal{E}_{\mathbf{k}})$ with $\Delta_{\mathbf{k}} = \Delta_{\text{var}}(\cos k_x - \cos k_y)$, $\xi_{\mathbf{k}} = \varepsilon_{\mathbf{k}} - \mu_{\text{var}}$, $\varepsilon_{\mathbf{k}} = -2(\cos k_x + \cos k_y) - 4t'_{\text{var}}\cos k_x \cos k_y$, and $\mathcal{E}_{\mathbf{k}} = -\sqrt{\xi^2_{\mathbf{k}} + \Delta^2_{\mathbf{k}}}$ [12,13]. The variational parame-

ters, all the independent pairs of $\alpha_{\rm var}^{ij}$, $\Delta_{\rm var}$, $\mu_{\rm var}$, and $t'_{\rm var}$, are determined by minimizing the variational energy: $E(\Psi_{\rm var}^{(N)}) = \langle\Psi_{\rm var}^{(N)}|H|\Psi_{\rm var}^{(N)}\rangle/\langle\Psi_{\rm var}^{(N)}|\Psi_{\rm var}^{(N)}\rangle$ for N even [14]. In this case $|\Psi_{\rm var}^{(N)}\rangle$ is a spin singlet and has a well-defined total momentum zero. Hereafter, the wave function with the optimized parameters is denoted by $|\Psi^{(N)}\rangle$, and $E^{(N)} = E(\Psi^{(N)})$. Also the energy unit (t) and the lattice constant a are both set to be one.

A single hole added to $|\Psi^{(N)}\rangle$ is naturally described by $|\Psi_{\mathbf{k}}^{(N-1)}\rangle = \hat{\mathcal{P}}_{N-1}\hat{\mathcal{P}}_G\hat{\mathcal{P}}_J\gamma_{\mathbf{k}\uparrow}^{\dagger}|\mathrm{BCS}\rangle$, where $\gamma_{\mathbf{k}\uparrow}^{\dagger}$ is the creation operator of the standard Bogoliubov quasiparticle with momentum $\mathbf{k}$ and $s =\uparrow$ [15]. The state with a single added electron, $|\Psi_{\mathbf{k}}^{(N+1)}\rangle$, is described in a similar way replacing $\hat{\mathcal{P}}_{N-1}$ by $\hat{\mathcal{P}}_{N+1}$. Note that these states have sharply defined $\mathbf{k}$, total spin $1/2$, and z component of total spin $1/2$. The use of these states is partially motivated by the diagonalization of H on small clusters—effort that indicated that the low-lying single-particle excitations are well described by a renormalized Bogoliubov quasiparticle state [16]—and partially on the recent proposal of a similar state [17]. The variational energies for these $(N \pm 1)$-electron states are denoted by $E_{\mathbf{k}}^{(N\pm1)}$. The single-particle excited states dispersion is thereby evaluated using $\varepsilon(\mathbf{k}) = E^{(N)} - E_{\mathbf{k}}^{(N-1)}$ $(E_{\mathbf{k}}^{(N+1)} - E^{(N)})$ for the one-electron removal (addition) spectrum [2].

In Fig. 1(a), as a typical example, the calculated dispersion $\varepsilon(\mathbf{k})$ in the nodal direction is shown for the 2D t-J model with $J/t = 0.3$ and $t'/t = -0.2$, at hole density $x = 1 - n = 0.099$. Here $n = N/L$ and L is the total size of the system. In the figure, the one-particle removal and additional spectra are denoted by open and solid marks, respectively. As seen in the figure, these spectra are almost symmetric in energy about the center of the dispersion. This might be expected because $|\Psi^{(N\pm1)}\rangle$ is made of a single Bogoliubov mode (with the projections), which shows a symmetric spectrum $\pm\mathcal{E}_{\mathbf{k}}$ [15]. From these results several important quantities are evaluated, such as the nodal Fermi momentum $[\mathbf{k}_{\rm F} = (k_{\rm F}, k_{\rm F})]$, Fermi energy $(E_{\rm F})$, bandwidth (W), as well as the nodal Fermi velocity at $\mathbf{k}_{\rm F}$ $(v_{\rm F})$.

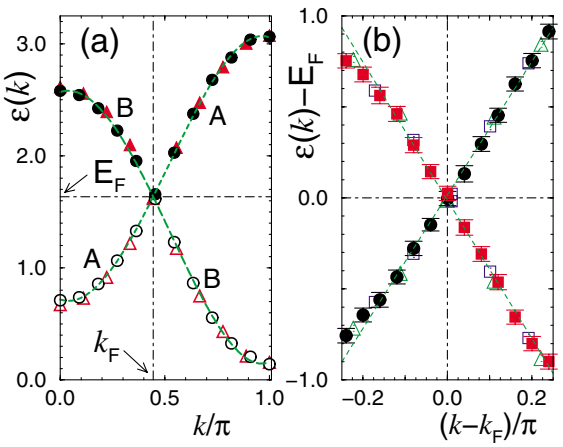

FIG. 1 (color online). One-particle dispersion $\varepsilon(\mathbf{k})$ in the nodal direction, $\mathbf{k} = (k, k)$, for the 2D t-J model with $J/t = 0.3$ and $t'/t = -0.2$, at $x = 0.099$. (a) Full dispersion for $L = 162$ (triangles) and 242 (circles). The one-electron removal (addition) spectrum is denoted by open (solid) symbols. The dashed (long dashed) line is a fitting curve of branch A (B) for the $L = 242$ data, using up to third-order polynomials. The estimated Fermi momentum and energy are indicated by $k_{\rm F}$ and $E_{\rm F}$, respectively. (b) Same as (a) but focusing on the excitations near $E_{\rm F}$. In addition to the data for $L = 162$ (open triangles) and 242 (open squares), results for $L = 1250$ (solid squares and circles) are also plotted. Dotted lines are a guide to the eye.

Let us refer to branch A as the main dispersion and to branch B as the "shadow" dispersion, since branch A (branch B) consists of all the one-electron removal (additional) states inside $k_{\rm F}^{\rm var}$, and all the one-electron additional (removal) states outside $k_{\rm F}^{\rm var}$. Here, $k_{\rm F}^{\rm var}$ is the nodal Fermi point of $|\mathrm{BCS}\rangle$ with the optimized parameters. Although this assignment is quite natural, we also calculated the quasiparticle weight directly and found that branch A has substantially more weight than branch B. The energy difference between $\mathbf{k} = (0, 0)$ and $\mathbf{k} = (\pi, \pi)$ in each branch naturally defines the bandwidth $W = \varepsilon(\pi, \pi) - \varepsilon(0, 0)$. Next, we fit the data in each branch using up to third-order polynomials. As shown in Fig. 1(a), the fitting is highly satisfactory. The intersection of the fitting curves provides the Fermi energy $E_{\rm F}$ and the nodal Fermi point $\mathbf{k}_{\rm F}$ [18]. From these fitting curves, we obtain the nodal Fermi velocity $v_{\rm F}$ at $\mathbf{k}_{\rm F}$.

The satisfactory fitting of the dispersions $\varepsilon(\mathbf{k})$ in the nodal direction already indicates that $\varepsilon(\mathbf{k})$ is a smooth function of $\mathbf{k}$ and, therefore, it suggests that the state used here does not have the kink structure observed experimentally. To study this in more detail, we calculated the nodal dispersion $\varepsilon(\mathbf{k})$ on a cluster with $L = 1250$, where the number of allowed $\mathbf{k}$ points in the nodal direction is 50 and, thus, the momentum resolution $\delta|\mathbf{k}|$ is about $0.18/a$ [19]. The results are presented in Fig. 1(b). It is fairly clear that the dispersions in both branches are almost linear around $E_{\rm F}$, and no kinklike structure is seen. If there were a kink structure in the dispersion, as observed experimentally, it would not be possible to fit the data for both one-electron removal and additional spectra using the same straight line. Comparing the data for $L = 1250$ and those for smaller systems shown in Fig. 1(b), it is apparent that the size dependence of the dispersion is small, and therefore we can safely estimate quantities such as $v_{\rm F}$ using the smaller systems.

Figure 2 summarizes the x dependence of various quantities for the 2D t-J model with $J/t = 0.3$ and $t'/t = -0.2$, which is a typical parameter set for the cuprates [2]. Figure 2(a) shows that $v_{\rm F}$ is weakly dependent on x up to about $x = 0.1$–0.2—with $v_{\rm F} \sim 0.8$–$1.0t$—and then increases with further increasing x. If $t \sim 500$ meV and $a \sim 4$ Å are used, the calculated value of this nearly x inde-

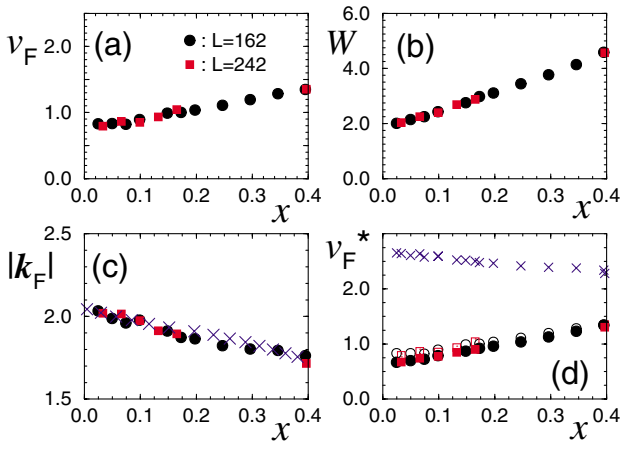

FIG. 2 (color online). (a) Nodal Fermi velocity v_F, (b) bandwidth W, (c) nodal Fermi momentum $|\mathbf{k}_F|$ (solid symbols), and (d) renormalized Fermi velocity v_F^* (solid symbols) (see text) for the 2D t-J model with $J/t = 0.3$ and $t'/t = -0.2$ at different x. For comparison, in (c) the free-electron nodal Fermi points (crosses) are also shown. In (d) the Fermi velocity for the free electrons v_F^0 (crosses) and v_F (open symbols) are also plotted.

pendent v_F corresponds to approximately 1.6–2.0 eV Å, which is compatible with ARPES data within the experimental error bars [6]. The present results are also consistent with recent reports by Paramekanti *et al.* [20,21], including the overall increasing behavior of v_F as a function of x [22].

In Fig. 2(b) and 2(c) the calculated bandwidth W and the nodal Fermi momentum k_F are shown, respectively. Although k_F approximately follows the result for free electrons (with t'), W has a stronger x dependence. It should be emphasized that this nontrivial x dependence of W is caused by strong correlations, which are imposed in the wave function by the Gutzwiller projection $\hat{\mathcal{P}}_G$. From Fig, 2(b), it is expected that the effective mass in the nodal direction monotonically increases with decreasing x, but it is finite even at $x \to 0$.

Now we show that the x dependence of v_F is understood quantitatively by a simple picture of a renormalized Fermi velocity. Since k_F is similar to the free electrons results (with t'), a natural procedure to follow is to calculate a renormalized Fermi velocity v_F^* from the value of the free electrons v_F^0 at k_F. In Fig. 2(d), $v_F^* = \gamma v_F^0$ is plotted, where $\gamma = W/W_0$ is a renormalization constant and $W_0 = 8t$ is the free electron's bandwidth. Clearly, v_F^* can now reproduce v_F for almost all the doping range studied.

To support this argument, systematic calculations are done for various model parameters, and the results are shown in Fig. 3(a)–3(d). It is apparent from the figures that v_F^* can indeed explain the x dependence of v_F quantitatively for a wide hole-doping range. The main features of the J and t' dependences are as follows: (i) v_F increases with J [Fig. 3(a) and 3(b)], and (ii) the increasing tendency of v_F with x weakens with $|t'|$ [Fig. 3(b)–3(d)]. These dependences can be explained by the renormalized velocity picture as well. While k_F does not depend on J [Fig. 3(f)] and, thus, neither does v_F^0 [Fig. 3(g)], W does depend on J and becomes larger with J [Fig. 3(e)]. Therefore v_F^* increases with increasing J. In contrast, t' does affect the value of v_F^0, and has a decreasing trend with increasing x [Fig. 3(g)]. Thus, v_F^* shows a reduced tendency to increase with x. Moreover, this decreasing trend can cancel the increasing behavior of W with x and, as a consequence, v_F^* can present a rather weak x dependence over a wide hole-doping range, as in Fig. 3(d), which agrees qualitatively with the calculated dependence of v_F. For comparison with experiments, we also show E_F for various t' in Fig. 3(h). The x dependence of E_F seems to be stronger for large $|t'|$ than for small $|t'|$, a trend that has been seen in experiments [23].

Even though our main goal is to study the low-lying excitations of the strongly correlated superconducting state, $|\Psi_{\mathbf{k}}^{(N\pm1)}\rangle$, it is interesting to consider the accuracy of our estimate of v_F for the 2D t-J model. To this end, we have carried out a fixed-node approximation Green function MC simulation using $|\Psi_{\mathbf{k}}^{(N\pm1)}\rangle$ as a guiding function

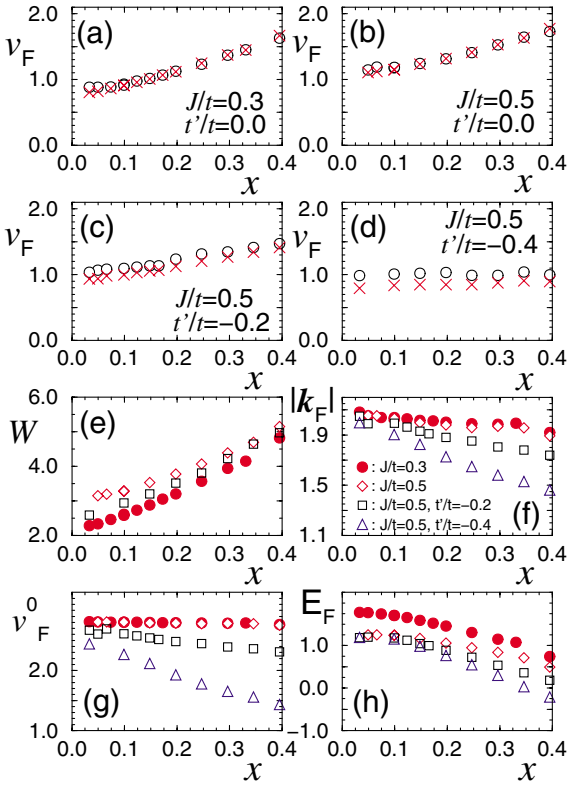

FIG. 3 (color online). (a)–(d) x dependence of the nodal Fermi velocity v_F (open marks) and the renormalized Fermi velocity v_F^* (crosses) for the 2D t-J model. The parameters used are indicated in the figures. (e)–(h) x dependence of W (e), k_F (f), the nodal Fermi velocity of the free electrons at $\mathbf{k}_F$ (g), and E_F (h) for the different parameters indicated in (f).

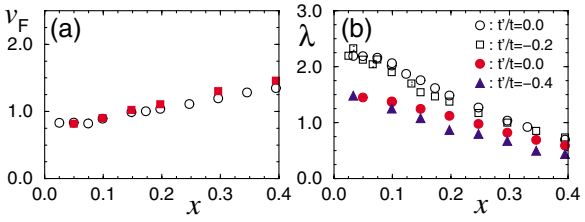

FIG. 4 (color online). (a) v_F vs x for the 2D t-J model with $J/t = 0.3$ and $t'/t = -0.2$ calculated using the Green function MC method with fixed-node approximation (solid symbols). For comparison, the variational estimates shown in Fig. 2(a) are also provided (open symbols). (b) x dependence of λ for $J/t = 0.3$ (open marks) and 0.5 (solid marks) with different t'/t.

[14]. As observed in Fig. 4(a), the calculated v_F compare well with the variational estimate.

Finally, we show in Fig. 4(b) a coupling strength defined as $\lambda = v_F^0/v_F - 1$ which is the first derivative of the real part of the single-hole self energy Σ' at E_F ($\lambda = -\partial\Sigma'(\omega)/\partial\omega|_{\omega=E_F}$) if the momentum dependence of Σ' is assumed weak [24–26]. It is interesting to note that λ seems to be determined largely by J, not by t', for a wide range of x, and becomes weakly depending on J and t' for $x \gtrsim 0.3$–0.35. This monotonically decreasing behavior with x as well as the value of λ are in good agreement with experimental estimates [5].

In conclusion, the low-lying one-particle excitations of a strongly correlated superconducting state was studied. It was found that the dispersion $\varepsilon(\mathbf{k})$ in the nodal direction shows a linear dependence for a wide range of excitation energies around E_F (~ 1.0–$1.5t$) and, thus, does not present a kinklike structure [27]. Systematic estimations are made for the nodal Fermi velocity v_F directly from the calculated $\varepsilon(\mathbf{k})$. The x dependence of v_F as well as λ are in good agreement with experiments. It is shown that the model parameter dependence of v_F is quantitatively explained by a simple picture of the renormalized Fermi velocity. Our results suggest that the kink structure observed experimentally is caused by other degrees of freedom not included in our study. Although the calculated $\varepsilon(\mathbf{k})$ in the nodal direction has no kink, the estimated v_F as well as the coupling strength λ compare well with ARPES experiments. These results lead us to the speculation that a major part of the low energy physics for the cuprates can still be described mainly by a purely electronic t-J-like model [28]. The ''universal'' Fermi velocity found in experiments [6] turns out to be explained here by a rather accidental compensation of two effects: the bandwidth W decreases with decreasing doping x due to correlation, while the bare Fermi velocity instead increases and further changes with t'/t. Therefore this effect might be less significant from the theoretical point of view, contrary to what was previously assumed. Our results indicate that more accurate experiments should eventually detect a ''nonuniversal'' and weakly doping dependent Fermi velocity.

We are grateful to C. Castellani, R. Hlubina, N. Nagaosa, and M. Randeria for helpful discussions. This work was supported in part by MIUR-COFIN 2003. E. D. was supported by NSF Grant No. DMR 0443144.

[1] J. G. Bednorz *et al.*, Z. Phys. B **64**, 189 (1986).
[2] See, e.g., E. Dagotto, Rev. Mod. Phys. **66**, 763 (1994).
[3] See, e.g., A. Damascelli, Z.-X. Shen, and Z. Hussain, Rev. Mod. Phys. **75**, 473 (2003).
[4] P. V. Bogdanov *et al.*, Phys. Rev. Lett. **85**, 2581 (2000).
[5] A. Lanzara *et al.*, Nature (London) **412**, 510 (2001); P. D. Johnson *et al.*, Phys. Rev. Lett. **87**, 177007 (2001).
[6] X. J. Zhou *et al.*, Nature (London) **423**, 398 (2003).
[7] See, e.g., M. Eschrig *et al.*, Phys. Rev. B **67**, 144503 (2003); S. Verga *et al.*, Phys. Rev. B **67**, 054503 (2003).
[8] F. C. Zhang *et al.*, Phys. Rev. B **37**, 3759 (1988).
[9] E. Dagotto and J. Riera, Phys. Rev. Lett. **70**, 682 (1993).
[10] S. Sorella *et al.*, Phys. Rev. Lett. **88**, 117002 (2002).
[11] C. Gros, Ann. Phys. (N.Y.) **189**, 53 (1989); H. Yokoyama and M. Ogata, J. Phys. Soc. Jpn. **65**, 3615 (1996), and references.
[12] To maximize available $\mathbf{k}$ points in the nodal direction, tilted lattices with size $L = m^2 + m^2$ (m, integer) and periodic boundary conditions are used [2]. To avoid a possible singularity in $f_{\mathbf{k}}$, a particle-hole transformation for electrons with down spin is used [H. Yokoyama and H. Shiba, J. Phys. Soc. Jpn. **57**, 2482 (1988)].
[13] To stabilize the numerical calculations, occasionally farther neighboring pairing functions are included in $|\Psi_{\rm var}^{(N)}\rangle$.
[14] S. Sorella, Phys. Rev. B **64**, 024512 (2001).
[15] See, e.g., J. R. Schrieffer, *Theory of Superconductivity* (Addison-Wesley, New York, 1988).
[16] Y. Ohta *et al.*, Phys. Rev. Lett. **73**, 324 (1994).
[17] R. B. Laughlin, cond-mat/0209269.
[18] k_F determined in this way is compatible with $k_F^{\rm var}$.
[19] Since we did not find a significant size dependence of the optimized variational parameters, the optimized parameters for $L = 242$ are used for $L = 1250$.
[20] A. Paramekanti *et al.*, Phys. Rev. Lett. **87**, 217002 (2001); Phys. Rev. B **70**, 054504 (2004).
[21] M. Randeria *et al.*, Phys. Rev. B **69**, 144509 (2004).
[22] The present work addressing v_F differs from the interesting previous studies by Paramekanti *et al.* [20,21] in the following: Here v_F is calculated directly from ε(k) while they estimate v_F from the discontinuity of the slope in the first moment of spectral function, a method which does not require the wave function for the excited state. Their variational state does not include $\hat{\mathcal{P}}_J$. The model they studied is the Hubbard model, not the t-J model.
[23] K. Tanaka *et al.*, cond-mat/0312575.
[24] See, e.g., G. D. Mahan, *Many Particle Physics* (Kluwer Academic, New York, 2000).
[25] See also A. A. Kordyuk *et al.*, cond-mat/0405696.
[26] By computing the quasiparticle weight, we have checked that this widely used assumption holds for $x \gtrsim 0.1$.
[27] For another point of view on the explanation of the kink, see Ref. [21].
[28] See, e.g., G.-H. Gweon *et al.*, Nature (London) **430**, 187 (2004).